

DISTRIBUTED SAMPLING AND RECONSTRUCTION OF NON-BANDLIMITED FIELDS IN SENSOR NETWORKS BASED ON SHIFT-INVARIANT SPACES

Günter Reise and Gerald Matz

Institute of Communications and Radio-Frequency Engineering, Vienna University of Technology
Gusshausstrasse 25/389, A-1040 Vienna, Austria; email: {greise,gmatz}@nt.tuwien.ac.at

ABSTRACT

We use the theory and algorithms developed for so-called shift-invariant spaces to develop a novel distributed architecture for sampling and reconstructing non-bandlimited fields in wireless sensor networks. Our scheme groups neighboring sensors into clusters that locally perform highly accurate field reconstruction with limited communication overhead. The overall complexity of our method scales only linearly with the number of sensors. Numerical simulations illustrate that the proposed field reconstruction scheme outperforms band-limited reconstruction, even though the latter has much larger complexity.

Index Terms— Wireless sensor network, field reconstruction, shift-invariant space, B-splines

1. INTRODUCTION

Wireless sensor networks (WSN) are becoming more and more popular as solution to distributed inference problems in quite diverse monitoring applications [1]. The basic idea is to use remote sensors, spatially distributed over the region to be monitored, to collect and process spatial measurements of a physical quantity of interest. In this paper, we are specifically concerned with the reconstruction of physical fields from irregular samples provided by the sensors. This problem has been previously addressed in the literature under the assumption that the field is strictly bandlimited (BL). An efficient scheme for the reconstruction of BL fields using a trade-off between spatial oversampling and sensor quantizer resolution was presented in [2]. The accuracy of BL reconstruction in WSN using linear filters and non-uniform sampling was studied using random matrix theory in [3]. In conventional temporal sampling applications, sufficient band-limitation is ensured by preceding the sampling with an analog anti-aliasing filter. With sensor networks, this is inherently impossible since the analog field cannot be accessed or pre-processed. At the same time, many physical fields are not a priori strictly BL. This was the motivation for [4] to analyze the errors incurred when using BL reconstruction in non-BL fields, showing that significant oversampling is required to achieve small reconstruction errors.

In this paper, we approach the non-BL field reconstruction problem in WSN from a different perspective. Specifically, we propose to use the theory and algorithms that have been developed for *shift-invariant spaces* [5] for the purpose of modeling, sampling, and reconstructing non-BL fields. A major advantage of this approach is the fact that shift-invariant spaces allow to model smooth functions (fields) without requiring strict band-limitation. In fact, non-BL shift-invariant spaces closely resemble non-wave fields (e.g., electrostatic, gravitation, diffusion in liquids and gases) like those considered in [6]. In addition, there exist efficient interpolation algorithms

both for regular and irregular sampling sets. Moreover, these algorithms are local in the sense that reconstructing the field at a certain spatial position requires only samples from a small neighborhood. We will demonstrate that all these properties render shift-invariant spaces inherently better suited for WSN applications than BL spaces. Specifically, we exploit the locality of shift-invariant spaces to reduce the communication and computational burden of field reconstruction. To this end, we develop a field reconstruction protocol based on a system architecture where the WSN is partitioned into clusters and a “cluster-head” performs local reconstruction using only samples obtained within its cluster. Here it is required that the positions of the sensors that provide samples are known to the cluster heads. Numerical simulations illustrate that our approach is superior to BL reconstruction in that it achieves smaller reconstruction errors with the same number of sensor or allows to deploy fewer sensors to achieve a prescribed reconstruction quality.

The remainder of the paper is organized as follows. In Section 2, we discuss shift-invariant spaces and their underlying generators. In Section 3 we introduce our system architecture. In Section 4, we outline the general approach for reconstruction in shift-invariant spaces and we then propose an efficient scheme implementing this reconstructions in a WSN assuming compactly supported generator functions. Section 5 illustrates the advantages of our approach via numerical simulations. Finally, Section 6 summarizes the main results.

2. SHIFT-INVARIANT SPACES

We first review some basic facts about shift-invariant spaces in two dimensions following [5] but using a terminology adapted to our WSN setup. A shift-invariant space $V(g)$ is a linear subspace of¹ $L^2(\mathbb{R}^2)$ comprising all fields that can be represented as weighted superposition of spatial translates of some generator function $g(x, y) \in L^2(\mathbb{R}^2)$, i.e.,

$$V(g) = \left\{ f \in L^2(\mathbb{R}^2) : f(x, y) = \sum_{(k,l) \in \mathbb{Z}^2} c_{k,l} g(x - kD_x, y - lD_y) \right\}.$$

where $c_{k,l} \in l_2(\mathbb{Z}^2)$. Without loss of generality, we will assume $D_x = D_y = 1$ throughout the paper, since this can always be ensured via an appropriate scaling of the spatial coordinates x and y . To guarantee the stability of the representation above, we further assume that the set of translates $\{g(x - k, y - l)\}_{(k,l) \in \mathbb{Z}^2}$ forms a Riesz basis for $V(g)$ [7].

¹Here, $L^2(\mathbb{R}^2)$ is the space of square-integrable fields on \mathbb{R}^2 , $\int_{\mathbb{R}^2} |f(x, y)|^2 dx dy < \infty$, and $l_2(\mathbb{Z}^2)$ is the space of square-summable sequences, $\sum_{k,l \in \mathbb{Z}} |c_{k,l}|^2 < \infty$.

Funded by FWF Grant N10606.

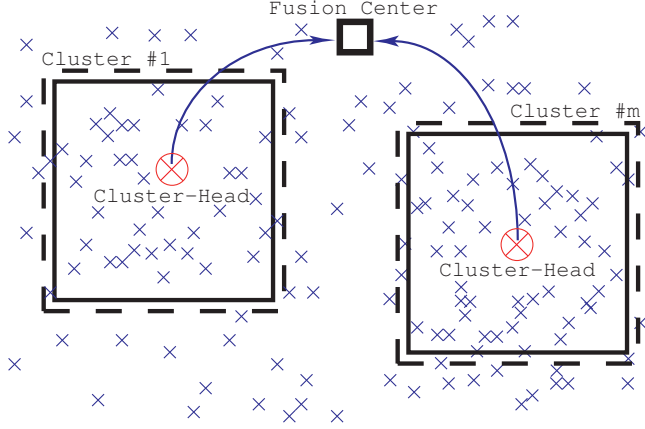


Fig. 1. WSN architecture for field reconstruction. The field is reconstructed locally within each cluster. If desired, the result is forwarded to the fusion centre.

We note that BL spaces are actually special cases of shift-invariant spaces, obtained with the separable sinc-type generator

$$g_{\text{BL}}(x, y) \triangleq \frac{\sin(B_x \pi x)}{B_x \pi x} \frac{\sin(B_y \pi y)}{B_y \pi y} \quad (1)$$

where B_x and B_y denote the spatial bandwidths. Note that (1) decays rather slowly. Hence, the corresponding space $V(g_{\text{BL}})$ is non-local, i.e., in the sampling/reconstruction problem the value of $f(x, y)$ depends on samples that are arbitrarily far away from (x, y) . This is clearly undesirable and motivates the use of generator functions with compact support, i.e., $\text{supp } g \subseteq [-S/2, S/2] \times [-S/2, S/2]$. Here, the support of $g(x, y)$ is defined as

$$\text{supp } g \triangleq \text{cl}\{(x, y) \in \mathbb{R}^2 : |g(x, y)| > 0\},$$

where $\text{cl}\{\cdot\}$ denotes topological closure. A particularly useful class of compactly supported generator functions is given by basis-splines (B-splines). Specifically, we will use two-dimensional spline functions in the following, constructed as $g_N(x, y) = \tilde{g}_N(x)\tilde{g}_N(y)$, with the one-dimensional splines of order N defined via the N -fold convolution

$$\tilde{g}_N(x) \triangleq \underbrace{\Pi(x) * \Pi(x) \dots * \Pi(x)}_{N \text{ times}}, \quad (2)$$

with the rectangular function $\Pi(x) = \tilde{g}_0(x)$ defined as

$$\Pi(x) \triangleq \begin{cases} 1, & |x| \leq \frac{1}{2}, \\ 0, & \text{else.} \end{cases}$$

The support of the two-dimensional splines is given by $\text{supp } g_N = [-S_N/2, S_N/2] \times [-S_N/2, S_N/2]$ with $S_N = N + 1$. Due to this compact support, the shift-invariant spaces $V(g_N)$ are not BL. It is interesting and important in our application context that $V(g_N)$ is *local*, i.e., according to the representation $f(x, y) = \sum_{k,l} c_{k,l} g_N(x - k, y - l)$, the field value $f(x_0, y_0)$ at any position (x_0, y_0) depends on at most $S_N^2 = (N + 1)^2$ coefficients.

3. WSN ARCHITECTURE

We consider a WSN consisting of I sensors/nodes, which are deployed over a certain region \mathcal{A} to monitor the physical field $f(x, y)$, assuming that $f(x, y) \in V(g)$ with compactly supported $g(x, y)$. The measurements taken by the sensors are noisy samples of the physical field $f(x, y)$, i.e., $f_i = f(x_i, y_i) + w_i$. Here, $(x_i, y_i) \in \mathcal{A}$ denotes the position of the i th sensor and w_i subsumes measurement and quantization noise. We consider a clustered system architecture (see Fig. 1) where the monitored region is divided into M subregions \mathcal{A}_m , $m = 1, \dots, M$, such that $\bigcup_{m=1}^M \mathcal{A}_m = \mathcal{A}$. These subregions may overlap and have different size. The sensors within each sub-area \mathcal{A}_m form a cluster \mathcal{C}_m .

Within each cluster there is one node which serves as cluster-head. The m th cluster-head collects the measurements from all nodes $i \in \mathcal{C}_m$ within its cluster and computes estimates $\hat{c}_{k,l}$ of the coefficients of $f(x, y)$ within \mathcal{A}_m according to the algorithm outlined in Section 4. This presupposes that the cluster-heads know the positions of all sensors within the cluster. We note that the case $M = 1$ corresponds to a centralized setup with a single fusion center.

The choice of the sub-regions \mathcal{A}_m is determined by the support $\mathcal{S} \triangleq \text{supp } g = [-S/2, S/2] \times [-S/2, S/2]$ of the generator function and by the sensor density. Specifically, the reconstruction algorithm outlined below requires that the number $I_m = |\mathcal{C}_m|$ of measurements (sensors) within \mathcal{A}_m must be larger than the number of field coefficients to be estimated (denoted J_m , see below). We note that for BL field reconstruction this condition can never be met (i.e., local reconstruction is impossible) due to the infinite support of $g_{\text{BL}}(x, y)$. Hence, BL fields require a centralized architecture (one “cluster” comprising all sensors).

Depending on the application, the estimated coefficients $\hat{c}_{k,l}$ can be used to reconstruct the field within each subregion. Alternatively, the cluster-heads can forward the coefficients to a fusion center that globally reconstructs the field. Some of the field coefficients may be calculated by more than one cluster. In this case, the fusion center may average the multiple coefficient estimates for improved performance.

We emphasize the distributed nature of our WSN architecture, i.e., only local communication and computation is required. Furthermore, if reconstruction fails for a certain cluster \mathcal{C}_m , this has only a local effect, i.e., it is still possible to reconstruct $f(x, y)$ within $\mathcal{A} \setminus \mathcal{A}_m$. Moreover, it will be seen below that with our model, the complexity of field reconstruction is extremely low, i.e., only *linear* in the number of measurements and quadratic in the size of the generator’s support.

4. FIELD RECONSTRUCTION

4.1. Reconstruction Scheme

By extending [7] to two dimensions, we next show how the field $f(x, y) \in V(g)$ can be reconstructed within one sub-region \mathcal{A}_m from a finite number $I_m = |\mathcal{C}_m|$ of (noisy) samples, assuming that their positions are known and that the generator is compactly supported. For simplicity of exposition, we assume rectangular sub-regions \mathcal{A}_m .

Since any field value is completely determined by a neighborhood corresponding to \mathcal{S} , reconstruction within \mathcal{A}_m only requires the coefficients $c_{k,l}$ lying within $\mathcal{A}_m + \mathcal{S}$. Correspondingly, least-

squares field reconstruction amounts to minimizing

$$\sum_{i \in \mathcal{C}_m} \left| \sum_{(k,l) \in \mathbb{Z}_m^2} c_{k,l} g(x_i - k, y_i - l) - f_i \right|^2. \quad (3)$$

Here, $g(x, y)$, (x_i, y_i) , and f_i are the known quantities and the optimum coefficients, denoted $\hat{c}_{k,l}$, have to be determined for $(k, l) \in \mathbb{Z}_m^2 \triangleq \mathbb{Z}^2 \cap (\mathcal{A}_m + \mathcal{S})$. The problem (3) leads to a system of linear equations (see below) whose solution requires at least $I_m \geq J_m \triangleq |\mathbb{Z}_m^2|$ measurements f_i to be obtained within \mathcal{A}_m . Once the optimum coefficients $\hat{c}_{k,l}$ have been computed, the field within \mathcal{A}_m can be reconstructed as

$$\hat{f}(x, y) = \sum_{k,l \in \mathbb{Z}_m^2} \hat{c}_{k,l} g(x - k, y - l), \quad (x, y) \in \mathcal{A}_m. \quad (4)$$

4.2. Matrix Formulation

We next provide a reformulation of field reconstruction in terms of matrices and vectors. Let (k_0, l_0) and (k_1, l_1) denote the smallest and largest indices, respectively, in \mathbb{Z}_m^2 such that $J_m = K(l_1 - l_0 + 1)$ with $K \triangleq k_1 - k_0 + 1$. We define the $I_m \times J_m$ matrix

$$[\mathbf{G}]_{j,n} = g(x_{i_j} - k_n, y_{i_j} - l_n), \quad (5)$$

where $i_j, j = 1, \dots, I_m$, denotes the indices of the sensors located in \mathcal{A}_m (i.e., $\mathcal{C}_m = \{i_1, \dots, i_{I_m}\}$), $k_n = k_0 - 1 + (n \bmod K)$, and $l_n = l_0 + \lfloor \frac{n-1}{K} \rfloor$ (here, $\lfloor t \rfloor$ denotes the largest integer not larger than t). We emphasize that \mathbf{G} will be a sparse matrix whenever \mathcal{A}_m is larger than \mathcal{S} . Indeed, $g(x_{i_j} - k_n, y_{i_j} - l_n) \neq 0$ only if $|x_{i_j} - k_n| \leq S/2$ or $|y_{i_j} - l_n| \leq S/2$, which can happen for at most $\lceil |\mathcal{S}| \rceil = \lceil S \rceil^2$ of the J_m elements in each row ($\lceil t \rceil$ is the smallest integer not smaller than t). Thus, only a fraction of roughly $|\mathcal{S}|/|\mathcal{A}_m|$ of the elements in each row of \mathbf{G} are non-zero.

Corresponding to (5), the measurements and unknown coefficients are arranged into respective vectors \mathbf{f} and \mathbf{c} according to

$$[\mathbf{f}]_j = f_{i_j}, \quad [\mathbf{c}]_n = c_{k_n, l_n}. \quad (6)$$

These definitions allow to rewrite the minimization problem (3) as

$$\hat{\mathbf{c}} = \arg \min_{\mathbf{c}} \|\mathbf{G}\mathbf{c} - \mathbf{f}\|.$$

The optimum coefficient vector $\hat{\mathbf{c}}$ is thus obtained as solution to the associated normal equations [8],

$$\mathbf{G}^H \mathbf{G} \hat{\mathbf{c}} = \mathbf{G}^H \mathbf{f},$$

i.e., $\hat{\mathbf{c}} = (\mathbf{G}^H \mathbf{G})^{-1} \mathbf{G}^H \mathbf{f}$. We note that this presupposes $\mathbf{G}^H \mathbf{G}$ to be invertible, which is just another consequence of the requirement that there have to be enough appropriately spaced samples available. Technically, the sensor positions (x_i, y_i) , $i \in \mathcal{C}_m$, have to form a stable sampling set [7]. For the one-dimensional case, stable sampling sets for B-spline spaces are well understood. This is not true for the two-dimensional case, where even in the BL case only probabilistic statements have been obtained recently [9].

4.3. Algorithm

In the following, we summarize all algorithmic steps necessary to perform field reconstruction and we give estimates of their computational complexity.

Preprocessing. Solving the normal equations requires computation of the positive semi-definite $J_m \times J_m$ matrix $\mathbf{T} = \mathbf{G}^H \mathbf{G}$:

$$[\mathbf{T}]_{n',n} = \sum_{j=1}^{I_m} g^*(x_{i_j} - k_{n'}, y_{i_j} - l_{n'}) g(x_{i_j} - k_n, y_{i_j} - l_n).$$

Here, superscript $*$ denotes complex conjugation. Due to the compact support of $g(x, y)$ and the corresponding sparsity of \mathbf{G} , it follows that \mathbf{T} is also sparse. Since \mathbf{T} is sparse and positive definite, the normal equations can efficiently be solved using a sparse LDL factorization [8], i.e., $\mathbf{T} = \mathbf{L}\mathbf{D}\mathbf{L}^T$. Both, the calculation and the factorization of \mathbf{T} need $\mathcal{O}(I_m \lceil S \rceil^4)$ operations. Note that the computation of \mathbf{T} requires only the sensor positions and the generator function and can hence be performed by the cluster-head in advance before any actual measurements f_i are obtained.

Field reconstruction. First, $\bar{\mathbf{f}} = \mathbf{G}^H \mathbf{f}$ is computed according to

$$[\bar{\mathbf{f}}]_n = \sum_{j=1}^{I_m} g^*(x_{i_j} - k_n, y_{i_j} - l_n) f_{i_j}$$

The sparsity of \mathbf{G} resulting from the compact support of $g(x, y)$ allows to perform this step with $\mathcal{O}(I_m \lceil S \rceil^2)$ operations. Finally, we solve the normal equations $\mathbf{T}\hat{\mathbf{c}} = \bar{\mathbf{f}}$ for $\hat{\mathbf{c}}$. Using the pre-computed sparse factorization of \mathbf{T} , this amounts to solving $\mathbf{L}\mathbf{D}\mathbf{L}^T \hat{\mathbf{c}} = \bar{\mathbf{f}}$ via forward elimination and back substitution [8]. The coefficients $\hat{\mathbf{c}}$ are therefore obtained with complexity $\mathcal{O}(I_m \lceil S \rceil^4)$. Finally, the field can be reconstructed at any point $(x, y) \in \mathcal{A}_m$ according to (4). This requires $\mathcal{O}(\lceil S \rceil^2)$ operations per spatial point.

5. NUMERICAL SIMULATIONS

We next present numerical results to illustrate the performance of our distributed sampling and reconstruction scheme. The simulated WSN was deployed over the square region $\mathcal{A} = [0, 10] \times [0, 10]$. We consider two different sensor placements: i) ideal placement on a regular rectangular lattice $(d_x k, d_y l)$ with $k, l \in \mathbb{Z}$; ii) placement on a regular rectangular lattice with jitter (the jitters were i.i.d. uniform within $[-d_x/4, d_x/4] \times [-d_y/4, d_y/4]$). Our WSN architecture used $M = 4$ clusters corresponding to the square sub-regions $\mathcal{A}_1 = [0, 5] \times [0, 5]$, $\mathcal{A}_2 = [5, 10] \times [0, 5]$, $\mathcal{A}_3 = [0, 5] \times [5, 10]$, and $\mathcal{A}_4 = [5, 10] \times [5, 10]$. Field reconstruction was performed using B-spline spaces $V(g_N)$ of various order N . For comparison, we show results obtained with a centralized architecture using BL interpolation in $V(g_{BL})$ for the whole region \mathcal{A} (with $g_{BL}(x, y)$ clipped to the region of interest). We emphasize that the complexity of the latter is much higher.

We first present results obtained with a WSN consisting of $I = 44^2$ sensors with jittered positions (note that the jittered positions still are accurately known by the cluster-heads). The fields $f(x, y) \in V(g_3)$ were generated with random i.i.d. normally distributed coefficients $c_{k,l}$. Fig. 2(a) shows the normalized mean square error² (MSE)

$$\text{MSE} = \frac{\mathbb{E}\{\|\hat{f} - f\|^2\}}{\mathbb{E}\{\|f\|^2\}} \quad (7)$$

versus the signal-to-noise ratio $\text{SNR} \triangleq \mathbb{E}\{|f(x, y)|^2\}/\mathbb{E}\{|w_i|^2\}$ for our distributed architecture using the correct generator $g_2(x, y)$ (thus $S = S_2 = 3$) and for a centralized architecture performing BL reconstructions using $g_{BL}(x, y)$ in (1) with $B_x = B_y = 1$. It is seen that our distributed scheme outperforms BL reconstructions for all

²Here, $\mathbb{E}\{\cdot\}$ denotes mathematical expectation (with respect to the random field and the random sensor positions).

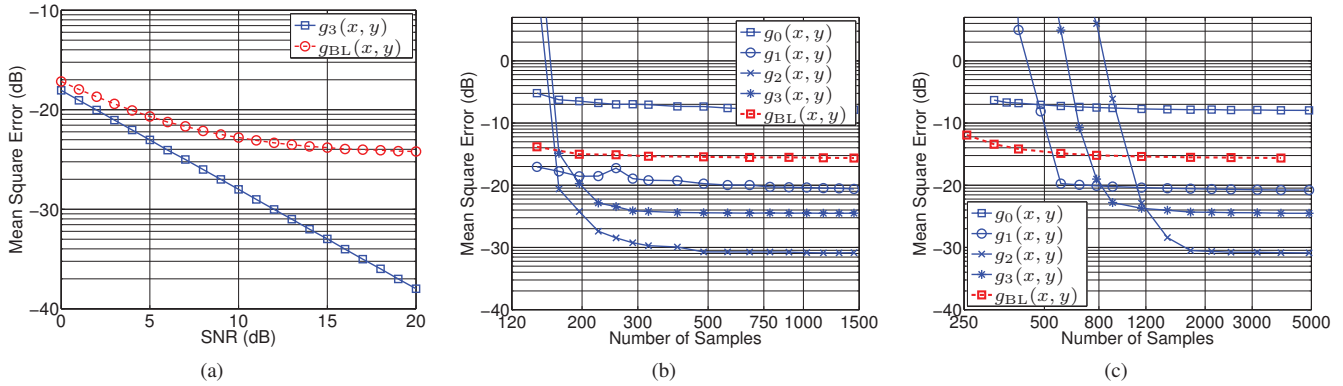


Fig. 2. Comparison of B-spline and BL interpolation: (a) MSE versus SNR for $I = 44^2$, (b) MSE versus number of regularly placed sensors at infinite SNR, (c) MSE versus number of sensors with jittered placement at infinite SNR.

SNRs in spite of its much lower complexity. In particular, the non-BL nature of the fields result in an error floor of BL reconstruction at high SNR (see Fig. 2(a)).

In a second example, we consider fields belonging to a shift-invariant space $V(\bar{g})$ induced by a Gaussian generator function, i.e.,

$$\bar{g}(x, y) = e^{-\lambda^2(x^2+y^2)}. \quad (8)$$

with $\lambda = 1.33$ (again, the true coefficients were i.i.d. normally distributed). Such spaces are useful models for diffusion fields (cf. [6]). We emphasize that the Gaussian generator is neither compactly supported nor BL. Our distributed scheme attempted reconstruction using B-spline generators with $N \in \{0, 1, 2, 3\}$. BL reconstruction was performed as before. In these experiments, infinite SNR was assumed (i.e., $w_i = 0$).

The reconstruction results in terms of MSE versus number of sensors I for ideal and jittered sensor placement are shown in Figs. 2(b) and (c), respectively. Note that even though there is no noise, all schemes feature an error floor which is due to the fact that none of the interpolation spaces is matched exactly to the fields under consideration. With ideal sensor placement and more than about $I = 160$ sensors, B-spline reconstructions outperforms BL interpolation for all orders except $N = 0$, with gains as high as 15 dB in the case of the optimal choice $N = 2$. It is also seen that the MSE obtained with $N = 4$ is higher than with $N = 2$, which can be attributed to oversmoothing.

Similar observations can be made for the case where the sensor positions are affected by jitter. Specifically, for dense networks with many sensors, B-spline reconstruction offers similar gains as in the case of ideal sensor placement. The major difference here is that for small number of sensors, the sensor positions more frequently do not provide a stable sampling set for the B-spline spaces, resulting in larger MSE. Note however that in these situations reconstruction typically fails locally, which is not reflected by our plots. Moreover, the computational complexity of our distributed architecture more than $I = 1000$ nodes is less than that of BL reconstruction using a few hundred sensors.

6. CONCLUSION

We proposed a cluster-based sensor network architecture for sampling and reconstruction of non-bandlimited fields. Our approach

builds on recent progress regarding non-uniform sampling in shift-invariant spaces. The major advantages of our scheme are excellent reconstruction quality, low computational complexity (linear in the number of sensors), and low communication overhead. In our future work, we plan to study the energy efficiency of our scheme (from a communication and computation perspective) in order to be able to choose the network and cluster size such that performance is optimized while guaranteeing maximum network lifetime.

REFERENCES

- [1] M. Gastpar, M. Vetterli, and P. L. Dragotti, "Sensing reality and communicating bits: a dangerous liaison," *IEEE Signal Processing Magazine*, vol. 23, no. 4, pp. 70–83, July 2006.
- [2] P. Ishwar, A. Kumar, and K. Ramchandran, "Distributed sampling in dense sensor networks: a 'bit-conservation principle'," in *Proc. IEEE Int. Symp. Information Processing in Sensor Networks*, Palo Alto, CA, April 2003, pp. 17–31.
- [3] A. Nordio, C. F. Chiasserini, and E. Viterbo, "Performance of linear field reconstruction techniques with noise and uncertain sensor locations," *IEEE Trans. Signal Processing*, vol. 56, pp. 3535–3547, Aug. 2008.
- [4] A. Kumar, P. Ishwar, and K. Ramchandran, "On distributed sampling of smooth non-bandlimited fields," in *Proc. IEEE Int. Symp. Information Processing in Sensor Networks*, Berkeley, CA, April 26–27, 2004, pp. 89–98.
- [5] A. Aldroubi and K. Gröchenig, "Nonuniform sampling and reconstruction in shift-invariant spaces," *SIAM Rev.*, no. 4, pp. 585–620, 2001.
- [6] Alex B. Gershman and Victor I. Turchin, "Nonwave field processing using sensor array approach," *Signal Processing*, vol. 44, pp. 197–210, 1994.
- [7] K. Gröchenig and H. Schwab, "Fast local reconstruction methods for nonuniform sampling in shift-invariant spaces," *SIAM J. Matrix Anal. Appl.*, vol. 24, no. 4, pp. 899–913, April 2003.
- [8] G. H. Golub and C. F. Van Loan, *Matrix Computations*, Johns Hopkins University Press, Baltimore, 3rd edition, 1996.
- [9] K. Gröchenig and R. F. Bass, "Random sampling of entire functions of exponential type in several variables," arXiv:0706.3818v2, 2008.